Diagnostics and Kinetic Modeling of the Ignition and the Extinction Transients of a Hollow Cathode N_2O Discharge

T. de los Arcos, C. Domingo, V. J. Herrero, M. M. Sanz,† and I. Tanarro*

Instituto de Estructura de la Materia (CSIC), Serrano 123, 28006 Madrid, Spain

Received: November 8, 1999; In Final Form: January 20, 2000

The present work describes the first experimental study of the transients involved in the turn on and off of a N_2O hollow cathode discharge until the attainment of the respective stationary states. Time-resolved Fourier transform infrared spectroscopy and quadrupole mass spectrometry with ionization by electronic impact have been used to measure the temporal evolution of the concentrations of the stable species present in the discharge N_2O, N_2, O_2, NO, and NO_2. A model based on a reduced set of kinetic equations gives a global account of the measured data; this model takes into account all the mechanisms considered in a former work (Arcos, T. et al. *J. Phys. Chem. A* **1998**, *102*, 6282) to explain the steady state of a continuous N_2O discharge but includes also additional mechanisms to which transient phenomena have proven to be much more sensitive than the stationary results. In particular, excitation of some vibrational levels of N_2O and homogeneous reactions of vibrationally excited species, as well as electron impact dissociation of the stable products of the discharge are considered. On the other hand, the partial formation of NO_2 by an heterogeneous reaction previously proposed seems to be confirmed.

1. Introduction

N_2O is used in various types of glow discharges that find widespread application in many scientific and technological fields, including spectroscopy, kinetics, and plasma-enhanced chemical vapor deposition (PECVD) (see references in ref 1). Despite the undoubted interest of the cold plasmas generated in glow discharges, the detailed kinetic modeling of these plasmas is still a major challenge, given the high number of interrelated concurrent processes and the lack of basic data about many of them. Radiofrequency (RF) discharges of N_2O were systematically studied by Cleland and Hess[2] and by Kline et al.[3] The two groups developed global kinetic models that were checked by monitoring some of the species present in the stationary discharge. Cleland and Hess[2] used Fourier transform infrared (FTIR) measurements of N_2O and NO, and Kline et al.[3] employed downstream mass spectrometric measurements of N_2O, NO, N_2, and O_2. These models include a large set of basic kinetic processes for the N_2O plasma and the mentioned authors discuss their relative relevance. Less exhaustive studies have also been published for microwave discharges of mixtures of N_2O with inert gases.[4,5]

In a previous work of our group, the stationary state of a DC hollow cathode N_2O discharge was experimentally characterized, and a kinetic model was proposed in order to explain the different concentrations of the involved molecular species found for different physical conditions.[1] This model took into account the kinetic mechanisms considered in the previous works on RF and MW, N_2O discharges, found in the literature,[2−5] and incorporated also some new heterogeneous reactions, mainly in order to explain the relatively high NO_2 concentration found in the DC hollow cathode discharge, and not observed in previous N_2O discharges.

All the studies commented on until now are restricted to the stationary state of the various glow discharges considered; however, the steady state condition is ultimately determined by a competition between processes having very different rates like electron dissociation and excitation, homogeneous, and heterogeneous reactions, convection, and diffusion. To investigate more accurately the kinetics of the plasma one should perform temporally resolved measurements with different time scales. In this respect, the study of transients associated with the ignition and the extinction of the discharge is a very useful tool to assess the actual contribution of the various kind of processes to the overall kinetics.

In the present work, "slow" transients are studied in the system. To that end, the hollow cathode discharge is turned on and off within a time interval of several seconds, long enough to guarantee that the respective stationary states are reached for all the chemical species involved in the process. As we shall see, this time scale will be of great help to clarify the relative influence of many of the relevant processes such as electron impact dissociation and homogeneous and heterogeneous reactions. Additional information can be obtained from the study of "faster" transients, as it will be demonstrated in a future paper,[6] where a 45 Hz square wave modulated N_2O discharge will be studied. With this modulation, time scales of a few ms can be reached and one can have access to the competition between processes of excitation, deexcitation and diffusion.

To achieve a characterization as complete as possible of the nitrous oxide plasma, FTIR absorption spectroscopy has been used for monitoring the temporal evolution of the concentration of the NO and NO_2 produced in the discharge, whereas the infrared inactive homonuclear products, N_2 and O_2, have been detected by mass spectrometry. The N_2O concentration has been determined also with both methods. To elucidate the most significant processes leading to the observed results, a simplified kinetic model is proposed, based on the numerical solution of

* Corresponding author. Fax: +34.91.5855184. E-mail: itanarro@iem.cfmac.csic.es.

† Universidad Alfonso X el Sabio, Villanueva de la Cañada, 28691 Madrid, Spain.

10.1021/jp993958t CCC: $19.00
Published on Web 04/27/2000

the time-dependent differential equations for the relevant species involved in the discharge.

2. Experimental Measurements

The detailed description of the hollow cathode discharge cell used in this work and of the method employed with the FTIR and the quadrupole mass spectrometers to characterize the discharge, when operated in the DC mode, is given elsewhere.[1,7] Briefly, the discharge cell was designed in our laboratory, easy to disassemble and with a symmetrical geometry of the electrodes, to be used for both mass spectrometry and FTIR emission and absorption spectroscopy. It consists of a cilindrical hollow cathode made of stainless steel, 90 mm long and with a 16 mm inner diameter, and two circular anodes of copper, each one of them placed at each end of the cathode at a distance of 25 mm and supported by an anode holder made of Pyrex and stainless steel. The discharge is fed by a 2000 V, 150 mA, square-wave modulated source, operative between 0 and 200 Hz. The electrodes are refrigerated by water. The discharge is sustained in a continuous and regulable flow of N_2O, evacuated by a rotary pump, and can be maintained stable approximately between 0.01 and 3 mbar. The cell was disassembled and cleaned carefully, including polishing of the electrodes, periodically, and no diferences were noticed in the experimental results obtained before and after each cleaning process. For absorption and emission measurements, a FTIR Bruker IFS66 spectrometer with both rapid-scan and step-scan options for the movable mirror was used. The detection of infrared inactive homonuclear species such as N_2 and O_2 generated in the discharge was done by means of a quadrupole mass spectrometer Balzers QMG112 working as a partial pressure detector, with electron impact ionization and a Faraday cup as the charge collector.

In the present work, the rapid-scan option of the FTIR spectrometer was used with a deuterated triglycine sulfate (DTGS) infrared detector to study, by time-resolved absorption spectroscopy, a single cycle of turning on and off the discharge. With a spectral resolution of 40 cm^{-1} and a mirror speed of 0.3 $cm.s^{-1}$, the minimum time required to perform a complete interferogram is ~42 ms, and taking into account the time interval between the end of a scan and the beginning of the following one, a temporal resolution of 100 ms was achieved. This resolution is enough to measure the transient phenomena of interest in the present work with a suitable level of detail. Two very different gas flow rates, 3 and 108 sccm, were characterized for an initial N_2O pressure of 2 mbar. The electrical power was 45 W. Each measurement was repeated two times and the agreement between them was very satisfactory. In this kind of experiments the interferograms were not averaged and thus, the noise level of the spectra was substantial; therefore, the relatively weak ($\nu_1 + 2\nu_2$) N_2O band, which was used in the DC discharge[1] to calibrate the absolute concentration values of N_2O, could not be used here for the 3 sccm gas flow rate, where the N_2O absorption signals are too small; instead, the absorption intensity of the more intense ν_3 band was employed. The intensity of this band versus the N_2O pressure without discharge was experimentally calibrated. The NO and NO_2 concentrations were calibrated as in the previous work,[1] by comparing the experimental data treated to simulate a transmittance spectra, with the simulated data obtained from the HITRAN database.[8]

The time resolution of the quadrupole mass spectrometer is determined by the gas residence time in the quadrupole vacuum chamber, which depends on its volume (3.5 L) and the pumping speed (300 L/s). In the present case this value is 12 ms. The temporal evolution of the N_2 and O_2 relative densities was measured with the quadrupole mass spectrometer synchronized to the m/q ratio of the respective parent ions, and collected by means of a digital oscilloscope working in the averaging mode. In the case of N_2, it was necessary the subtraction of a portion of the signal corresponding to a fragment of the parent ion, N_2O, at $m/q = 28$, which was a time dependent function. At the highest gas flow rates, the mass spectrometric signals of N_2 and O_2 were buried in noise. The NO signals could not be recovered suitably by mass spectrometry, due to the high contribution of the $m/q = 30$ peak from the fragmentation of N_2O. The FTIR and mass spectrometric results are shown in Figures 1 and 2, respectively. Electron densities and mean electron energies were taken from double Langmuir probe measurements of the continuous N_2O discharge[1] and were assumed to reach the stationary state almost instantaneously, in comparison with the time scales of the present work.[9]

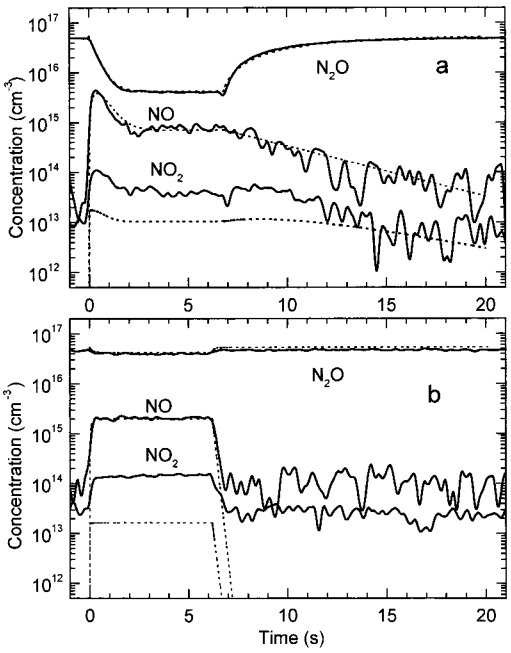

Figure 1. Time dependence of the absolute concentration of N_2O, NO, and NO_2, during the turn on and off of the discharge. The experimental data obtained by rapid-scan FTIR absorption spectroscopy are compared with the predictions of the present kinetic model. N_2O starting pressure, 2 mbar; electrical power, 45 W. (a) N_2O flow rate: 3 sccm. (b) N_2O flow rate: 108 sccm.

3. Chemical Kinetics Model

In our previous article[1] a kinetic model accounting basically for the stationary concentrations of the stable species appearing in a DC hollow cathode N_2O discharge was reported. In the present work, this model has been improved in an attempt to describe the transient effects observed when turning on and off the N_2O discharge, with a frequency of modulation low enough to allow for the establishment of the respective stationary states.

The inadequacy of the previous kinetic model derived from steady state data for the description of the transients investigated in the present work is clearly exemplified in Figure 3, where the measured time evolution of the concentration of nitrogen oxides after switching on and off the discharge is shown together with the model predictions for a slow (3 sccm) N_2O flow. As can be seen, only the evolution of the N_2O precursor is reproduced satisfactorily, but neither the initial rise nor the subsequent decay of the NO and NO_2 concentrations can be accounted for by the model.

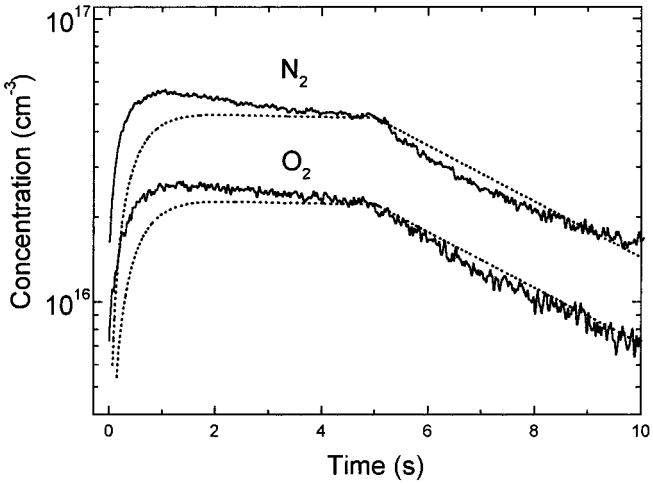

Figure 2. Temporal evolution of the concentration of N_2 and O_2 during the turn on and off of the hollow cathode N_2O discharge, obtained by mass spectrometry. The intensities of the experimental signals have been scaled to the predictions of the present kinetic model. N_2O starting pressure, 2 mbar; electrical power, 45 W. N_2O flow rate: 3 sccm.

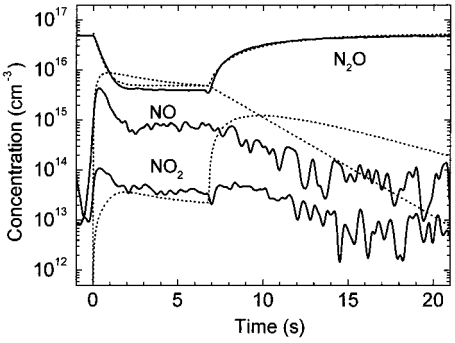

Figure 3. Temporal variation of the absolute concentrations of the nitrogen oxides N_2O, NO and NO_2 during the turn on and off of the hollow cathode N_2O discharge, compared with the predictions of the kinetic model of ref 1, based on steady-state data. N_2O starting pressure, 2 mbar; electrical power, 45 W. N_2O flow rate: 3 sccm.

The new model contains all the chemical reactions considered in the former one, although some of the rate coefficients have been revised. In addition, some physicochemical processes, which have been revealed to be crucial for the satisfactory reproduction of transient effects, have been included. The previous steady state data are nearly insensitive to the inclusion of these new processes in the model over the range of physical conditions where the discharge has been characterized. These results stress the importance of time-resolved measurements for the elucidation of the contribution of particular mechanisms to the kinetics of this kind of systems.

The kinetic model finally presented here describes not only the present experimental measurements, but also the steady-state DC discharge[1] and is compatible too with the faster transient data obtained with a higher modulation frequency of the discharge which will be described in a forthcoming paper,[6] although in that case diffusion effects should be taken into account in detail.

The main modifications of the present work are now advanced briefly: the electron impact excitation of some vibrational N_2O stretching modes and some of their deexcitation pathways are included, and at the same time the reactivity of N_2O homogeneous reactions is considered to be increased when some of these excited levels are involved. Besides, the electron impact dissociation of all the stable molecules of the discharge except

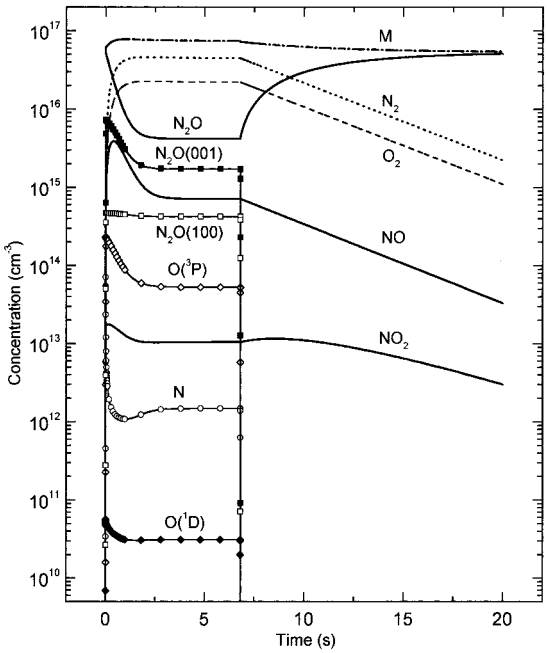

Figure 4. Theoretical predictions of the temporal evolution of the concentrations of all the species involved in the chemical kinetics model for the ignition and extinction of a N_2O hollow cathode discharge operating at 2 mbar, 45 W, and 3 sccm. The stable species are considered to be homogeneously distributed along the whole cell, concentrations of transient species are considered to be significant only in the plasma volume (see text).

N_2 is incorporated to the model. On the other hand, the relative importance of some heterogeneous reactions is modified after an inspection of the time evolution of the relevant concentrations when the discharge is turned off.

In a way similar to that in ref 1 and in previous works dealing with the stationary state of N_2O glow discharges,[2−5] diffusion effects have not been considered here because the transients of interest in the present work are still slow enough to justify the assumption of stable species being well mixed and occupying all the reactor volume. Short lived species, however, are actually considered to be confined to the plasma region.

The results of the application of the present model to the conditions of our discharges and its comparison to the time-resolved measurements of this work is shown in Figures 1, 2, and 4. The predictions of the model for steady-state conditions are compared in Figure 5 to the experimental data. In the following, we comment on the various types of dynamic processes that have been considered.

Dissociation Processes. Electron impact dissociation of N_2O in the plasma volume is the key process in the chemical kinetics of the discharge and the main cause of the decrease of N_2O concentration when the discharge is turned on. As can be seen in Table 1, three N_2O electron dissociation channels have been considered, two of them producing $N_2 + O$, but with the oxygen atoms in its fundamental, ^3P, or in the excited, ^1D state (reactions D_1 and D_2), and the last one producing NO + N (reaction D_3). This latest reaction was not included in the previous work[1] because NO and N are known to react very quickly through the homogeneous reaction $NO + N \rightarrow N_2 + O(^3P)$, which now is also included in the model (reaction G_7), and could be considered as intermediate stages of the first dissociation channel. In the steady-state model, the inclusion of the two reactions did not lead to appreciable differences; nevertheless, both of them are taken into account in the present work, due to their possible influence on transient effects. The respective rate

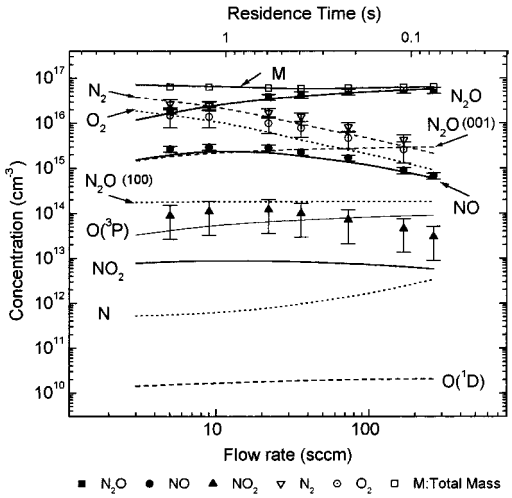

Figure 5. Comparison between the measured concentrations of the species involved in a (symbols) N_2O continuous discharge operating at different gas flow rates[1] and the theoretical results obtained with the (lines) present kinetic model. The discharge was maintained at a pressure of 2 mbar, with an electrical power of 15 W.

constants for the three N_2O dissociation reactions by electronic impact have been assumed to be 8×10^{-10}, 3.7×10^{-10}, and 1.2×10^{-10} cm^3 molecule^{-1} s^{-1}. Since rate constants for electron impact dissociation at low energies are not available in general, the former ones have been calculated in this work using a method similar to that described in ref 1 for a continuous discharge. The sum of the three rate constants is chosen in order to reproduce the experimental ground-state N_2O concentration when the discharge is on, and the values of the individual rate constants are adjusted to account appropriately for the N_2 and NO stationary concentrations.

In the present work, the excitation of some N_2O vibrational levels by electronic impact has been taken into account. They were not included in our previous work on DC N_2O discharges but have been included here, mainly because a high population ($\sim$9%) of N_2O in the weakly collisionally coupled (001) asymmetric stretching mode was observed by emission measurements.[7] Similar percentages of (001) population were obtained by other authors in previous spectroscopic studies of N_2O glow discharges.[10,11] Since the incorporation of N_2O excitation rate constants originates a slight depletion of the N_2O molecules remaining in the fundamental state and since a third dissociation channel has been included here, the revised values of the N_2O dissociation rate constants are slightly different than those assumed in ref 1. Nevertheless, these rate constants agree quite well with those proposed by Cleland and Hess[2] and are slightly smaller than the estimates of Kline et al.[3] for N_2O dissociation rate constants in a glow discharge plasma with a higher mean electron energy. On the other hand, the same rate constant values are assumed for dissociation processes of excited N_2O molecules, since the energies required to dissociate the vibrationally excited N_2O molecules are only 7−15% smaller than that required from the N_2O ground state.

Dissociation by electronic impact of NO and NO_2, appearing as stable products in the N_2O discharge, has been included in the present model with the rate constants shown in Table 1 (reactions D_4 and D_5). The bond strengths of these molecules are 6.5 and 3.1 eV, respectively.[12] The inclusion of a NO dissociation term is crucial in order to account for the time evolution of the NO concentration during the beginning of the discharge, as it will be shown later. Its rate constant has been estimated in order to fit the NO concentration when the stationary state of the discharge on is reached and the resulting value is very similar to that assumed by Kline et al.[3] The NO_2 dissociation rate constant has been assumed to be similar to that of NO and its inclusion leads to a better agreement with the observed evolution of the NO_2 concentration at the beginning of the discharge.

The dissociation of molecular oxygen, with a bond energy of 5.11 eV,[12] is assumed to happen through two possible channels, one of them (reaction D_6) giving rise to two oxygen atoms in their fundamental state, and the other one (reaction D_7) producing one of the oxygen atoms in its electronically excited ^{1}D level, as shown in Table 1. The ratio between the respective rate constants agrees with that found in the literature.[3,12] In any case, the sum of the two dissociation rates assumed in the present model is smaller than the assumed values

TABLE 1: Reactions Included in the Kinetics Model of the N_2O Hollow Cathode Discharge[a]

	reaction	rate constant	ref
	Disocciation by Electronic Impact		
D_1	$N_2O + e^- \rightarrow N_2 + O(^3P) + e^-$	8.0×10^{-10}	*b*
D_1	$N_2O(001) + e^- \rightarrow N_2 + O(^3P) + e^-$		
D_1	$N_2O(100) + e^- \rightarrow N_2 + O(^3P) + e^-$		
D_2	$N_2O + e^- \rightarrow N_2 + O(^1D) + e^-$	3.7×10^{-10}	*b*
D_2	$N_2O(001) + e^- \rightarrow N_2 + O(^1D) + e^-$		
D_2	$N_2O(100) + e^- \rightarrow N_2 + O(^1D) + e^-$		
D_3	$N_2O + e^- \rightarrow NO + N + e^-$	1.2×10^{-10}	*b*
D_3	$N_2O(001) + e^- \rightarrow NO + N + e^-$		
D_3	$N_2O(100) + e^- \rightarrow NO + N + e^-$		
D_4	$NO + e^- \rightarrow N + O(^3P)$	8.5×10^{-10}	*b*
D_5	$NO_2 + e^- \rightarrow NO + O(^3P) + e^-$	8.5×10^{-10}	*b*
D_6	$O_2 + e^- \rightarrow 2\,O(^3P) + e^-$	4.8×10^{-11}	*b*
D_7	$O_2 + e^- \rightarrow O(^3P) + O(^1D) + e^-$	7.2×10^{-11}	*b*
	Electronic Impact Excitation		
E_1	$N_2O + e^- \rightarrow N_2O(001) + e^-$	1.4×10^{-8}	*c*
E_2	$N_2O + e^- \rightarrow N_2O(100) + e^-$	1.4×10^{-8}	*c*
	Quenching of Excited States		
Q_1	$N_2O(001) + N_2O \rightarrow 2\,N_2O$	2.44×10^{-14}	7
Q_2	$N_2O(100) + N_2O \rightarrow 2\,N_2O$	5.26×10^{-13}	14
Q_3	$O(^1D) + N_2 \rightarrow O(^3P) + N_2$	2.6×10^{-11}	16
Q_4	$O(^1D) + NO \rightarrow O(^3P) + NO$	1.5×10^{-10}	17
	Homogeneous Reactions		
G_1	$N_2O + O(^1D) \rightarrow 2\,NO$	7.2×10^{-11}	16
G_1	$N_2O(001) + O(^1D) \rightarrow 2\,NO$		
G_1	$N_2O(100) + O(^1D) \rightarrow 2\,NO$		
G_2	$N_2O + O(^1D) \rightarrow N_2 + O_2$	4.4×10^{-11}	16
G_2	$N_2O(001) + O(^1D) \rightarrow N_2 + O_2$		
G_2	$N_2O(100) + O(^1D) \rightarrow N_2 + O_2$		
G_3	$N_2O(001) + O(^1D) \rightarrow NO_2 + N$	1.0×10^{-10}	*b*
G_4	$NO + O(^3P) + M \rightarrow NO_2 + M$	10^{-31}	16
G_5	$NO_2 + O(^1D) \rightarrow NO + O_2$	3.0×10^{-10}	*b*
G_6	$NO_2 + O(^3P) \rightarrow NO + O_2$	9.7×10^{-12}	16
G_7	$NO + N \rightarrow N_2 + O(^3P)$	3.0×10^{-11}	34
G_8	$NO + O(^1D) \rightarrow O_2 + N$	8.5×10^{-11}	34
	Heterogeneous Reactions		
W_1	$O(^1D) + \text{wall} \rightarrow O(^3P)$	2200	*d*
W_2	$O(^3P) + \text{wall} \rightarrow O(S)$	2200	*d*
W_3	$O(^3P) + O(S) \rightarrow O_2$	180	2
W_4	$N + \text{wall} \rightarrow (1/2)\,N_2$	16.1	*d*
W_5	$N_2O(001) + \text{wall} \rightarrow N_2O$	222	*d*
W_6	$N_2O(100) + \text{wall} \rightarrow N_2O$	222	*d*
W_7	$NO + O(S) \rightarrow NO_2$	2.75×10^{-3}	*b*
	Radiative Deexcitation		
R_1	$N_2O(001) \rightarrow N_2O$ ($\tau_1 \sim 4$ ms)	258	7
R_2	$N_2O(100) \rightarrow N_2O$ ($\tau_2 \sim 83$ ms)	12	22

[a] Rate Coefficients are in units of cm^3 molecule^{-1} s^{-1} for dissociation by electronic impact and bimolecular reactions. cm^6 molecule^{-2} s^{-1} for trimolecular reactions and s^{-1} for heterogeneous Reactions [b] Estimated in this work. [c] Calculated from ref 15. [d] Calculated for our cell geometry assuming $\gamma = 1$ (see text).

for NO and NO_2. No theoretical or experimental absolute values have been found for these rate constants at low electron energies but in some tests performed in our laboratory with pure O_2 discharges, a very low dissociation efficiency, lower than 1%, was found for physical conditions analogous to those of the N_2O discharges. Similarly, a very small amount of N_2 dissociation was experimentally obtained with a N_2 hollow cathode discharge, and N_2 dissociation has not been included in the model because its bond strength is 9.76 eV, notably higher than the mean electron energy measured in the plasma (~3 eV) and its relative dissociation rate constant is known to be much lower than that of O_2 for low electron energies.[13] Ionization processes by electronic impact are not included in the present model, in a way similar to refs 1 and 2, since reactions including ions were shown not to affect significantly the concentrations of the precursor and products in other N_2O discharges,[3] when they were included in the corresponding kinetic model.

Excitation Processes. In the present model, vibrational excitation of the weakly collisionally coupled (001) asymmetric stretching mode of N_2O by electron impact has been included (reaction E_1), to explain the high population in excited levels of this mode observed by emission measurements in the hollow cathode discharge, equivalent to a (001) vibrational temperature of ~1300 K. This fact originates a slight but noticeable depletion in the population of N_2O in its ground state which is observed by absorption spectroscopy. In the same way, excitation of the (100) symmetric stretching has been included too (E_2), since its excitation rate constant is quite similar to that of the (001) mode for the electron energy distribution considered in the present work; however, the (100) mode is known to relax by collision impact much faster than the (001) one.[11,14] The rate constant for N_2O excitation to the vibrational mode (001) is assumed to be 1.4×10^{-8} cm^3 molecule^{-1} s^{-1}. This rate constant has been calculated from the work of Hayashi et al.,[15] where the cross sections for the different processes originated by electron impact on N_2O are reported as a function of electron energy. Following Hayashi et al., the cross section for the excitation of the (001) mode has a maximum of 1.5×10^{-16} cm^{-2} at 2.5 eV. The electron energy distribution inside the cathode of our discharge is assumed to be of the Maxwell type, its mean energy, measured with a double Langmuir probe,[1] is 2.8 ± 0.5 eV and is thus close to that of the maximum in the excitation cross section. An upper limit for the rate constant reported here has been estimated roughly by assuming that all the electrons have a uniform kinetic energy close to 2.5 eV, and a cross section equal to the above-mentioned maximum value.

The rate constant assumed for N_2O excitation to the symmetric stretching mode, (100), has been estimated in a way similar to that of (001) and has the same value. The cross section for the excitation of this mode has also a peak at 2.5 eV, with a broader distribution, but a very similar maximum value (1.4×10^{-16} cm^{-2}) than that of (100).[15]

Other vibrational or electronic excitation paths have not been considered here because their excitation cross sections by electron impact within the interval of electron energies involved in the present work are much smaller than those of (100) or (001).[15] Furthermore, deexcitation by emission or quenching from these levels are very fast, so their populations are very small and do not contribute significantly to the depletion of the ground state of N_2O during the discharge. Rotational excitation has not been included because its relaxation can be assumed to happen instantaneously in comparison with the time scale of the present work, and because the broadening of the infrared bands during the discharge has been observed to be in fact small.

Deexcitation. The most significant excited species involved in the kinetics of the N_2O discharge is the metastable O(^{1}D). It is produced in the electron impact dissociation of N_2O and, besides its active participation in the chemical kinetics of the plasma, it is known to be efficiently quenched through inelastic collisions with the N_2 and NO molecules appearing as products of the N_2O discharge. Rate coefficients for these O(^{1}D) quenching processes included in the model (reactions Q_3 and Q_4) and shown in Table 1 have been obtained from refs 16 and 17, respectively. These coefficients, as well as those of homogeneous reactions where O(^{1}D) is involved, are high enough to make diffusion of the excited atoms outside the plasma volume negligible.

To explain the deexcitation of the vibrational excited levels (001) and (100) of N_2O, three kind of processes have been considered: spontaneous emission, quenching with N_2O in its ground state, and diffusion outward the plasma volume with possible deexcitation by collision on the wall. Self-absorption effects, which would populate secondarily these vibrational levels and extend their effective lifetimes, are not included, since changes in the ratios of the intensities of the more intense spectral lines were not observed when emission was detected through an optical path length twice the original one, with a mirror placed behind the rear window of the hollow cathode discharge cell.

The lifetime for spontaneous emission of the ν_3 band (R_1) starting from the (001) vibrational level was measured to be 4 ms,[7] in good agreement with other values found in the literature.[18] The quenching rate constant of this stretching mode by collision with N_2O in its ground state (reaction Q_1) has been taken from the Stern−Volmer plot of the (001) emission decay, obtained by emission measurements in a 45 Hz N_2O discharge at different N_2O flow rates (and consequently, different N_2O concentrations), made in our laboratory.[7] The resulting value, 2.44×10^{-14} cm^3 molecule^{-1} s^{-1}, is in approximate good agreement with Bates et al.,[10] who measured it by means of laser-induced fluorescence, and with previous works,[19,20] and it corresponds to a large mean collision number (~8000) which implies that the asymmetric stretching mode is only weakly collisionally coupled to other levels in this molecule, although several overtone and combination states of the symmetric stretch and bend lie close in energy to the 00°1 state. In this way, molecules excited within this manifold survive for a time interval comparable to the lifetime for spontaneous emission, which is long enough to diffuse from the plasma volume to the walls of the cathode (diffusion time ~1 ms) and even to be promoted to successively higher levels, hence the high (001) vibrational temperatures found in the present work (1300 K) and in refs 11 and 21. Diffusion effects will be considered in more detail in the section of heterogeneous reactions.

The N_2O symmetric stretching mode (100) has a lifetime for spontaneous emission, corresponding to the ν_1 band,[22] of 83 ms (reaction R_2), markedly larger than that of (001), so apparently this level should persist longer than the latest one; nevertheless, its quenching rate constant, 5.26×10^{-13} cm^3 molecule^{-1} s^{-1} (ref 14), implies a mean collision number of only ~300 collisions (reaction Q_2) and it relaxes much faster than the (001) mode at the pressures of the present experiments (relaxation time ~70 μs with 1 mbar of N_2O). Therefore, (100) vibrational temperatures not higher than 300−350 K are usually observed.[10,21] On the other hand, no diffusion to the surroundings

need to be considered for this level, since it deexcites fast enough to be present only in the plasma volume.

In general, throughout this work, the ground-state N_2O and the vibrationally excited stretching modes $N_2O(100)$ and $N_2O(001)$ will be treated as separate species.

Homogeneous Reactions. In the comparatively low-pressure plasma of the hollow cathode discharge, atom−molecule bimolecular reactions with significant participation of excited-state species are predominant. The set of homogeneous reactions considered here includes all those from the previous model[1] and incorporates a few new ones. In both models just one three body gas-phase reaction has been included. In addition, slight modifications of the former rate coefficients, in agreement with more recent data found in the literature, have been taken into account. The whole set of rate constants used can be found in Table 1 and the original bibliographic sources are cited in the fourth column of this table. Room-temperature rate coefficients have been considered, in accordance with the "cold" character of the hollow cathode glow discharge. All the homogeneous reactions are assumed to be irreversible, this assumption being justified by comparison of the reverse and forward rate constants.[17,23]

Because of its large activation energy,[24] the reaction of ground-state oxygen atoms $O(^3P)$ with N_2O plays no significant role in the plasma kinetics and has been consequently ignored. However, the reactions of nitrous oxide with $O(^1D)$ are certainly relevant. The two major exit channels of the $O(^1D) + N_2O$ reaction lead to 2NO and $N_2 + O_2$ respectively (reactions G_1, G_2). As indicated above, the evolution of ground-state N_2O and that of the vibrationally excited (100) and (001) modes are considered separately and, for each channel, the rate coefficient has been assumed to be the same for the three cases. Although no specific rate constants have been found in the literature for these reactive channels with vibrationally excited N_2O, this assumption is reasonable since the two exit channels considered have no barrier or a very small one[25] and vibrational excitation of N_2O is not expected to increase their reactivity.

The rest of the possible exit channels of $O(^1D)$ with ground-state N_2O should play a very minor role; in fact an upper limit of a few percent, as compared with the two major channels just commented on, has been estimated for the global reactivity of all of them.[26] However, in an attempt to explain the NO_2 concentration experimentally found in our hollow cathode discharge, too high in comparison with other N_2O discharges[2,3] where it was not detectable at all, we have assumed that the vibrational excitation of N_2O can enhance markedly the reactivity of the exit channel leading to the formation of NO_2. In our former work,[1] a possible heterogeneous reaction was invoked as the main source of the observed NO_2, but the evolution of the NO_2 concentration predicted with this hypothesis is clearly at variance with the present time-resolved experiments (see Figure 3 and the discussion on heterogeneous reactions below). In the present study we have included the reaction G_3 between the N_2O molecules excited to the long-lived, highly populated, (001) vibrational mode and the $O(^1D)$ atoms: $N_2O(001) + O(^1D) \rightarrow N + NO_2$. No direct information is available for this reaction and we have assumed a high rate constant for it in order to account better for the measured data. The effect on the kinetic model has been a considerable increase in the calculated NO_2 concentrations, approximating it more satisfactorily to the stationary values and to the temporal behavior of the experimental data, without further appreciable influences on the rest of the stable species appearing in the discharge. This channel is spin forbidden, but other spin forbidden processes have been shown to play an important role in the kinetics of the N_2O plasma.[5] In the present case, an upper limit of $\sim 10^{-12}$ cm^3 molecule^{-1} s^{-1} was estimated by Davison et al.[26] for the room-temperature rate constant of the reaction with ground-state molecules, $O(^1D) + N_2O \rightarrow N + NO_2$. The rate constant proposed in the present model for the $N_2O(001)$ reaction is about 2 orders of magnitude higher. This is not unreasonable. The beneficial effect of vibrational excitation for reactions with suitable barriers on their potential surfaces is well-known (see refs 27−29 and references therein). In fact, enhancements of more than 2 orders of magnitude in the comparative effect of reagent vibrational energy versus relative translational energy upon the reaction cross sections are well documented for some of the most prototypic A + BC reactions,[30,31] and the effect of vibrational excitation could be even more important for reactions with polyatomic molecules, where lower vibrational modes are accessible.[32] Unfortunately, the potential surface for this reaction pathway is largely unknown and one can only speculate with the existence of a suitable barrier. In the absence of more direct evidence, the incorporation of this process as source of NO_2 to the kinetic model is thus only a tentative hypothesis mainly justified by the better accordance with the data and should be taken with caution. On the other hand, the present results invite further theoretical and experimental investigation about the role of vibrational excitation on the $O(^1D) + N_2O$ reaction.

In comparison with the former process, reaction G_4 between NO and $O(^3P)$ in the presence of a third body represents a minor contribution to NO_2 production, but it has been included here, in the same way as it was included in the modeling of the DC discharge[1] and in previous works on N_2O microwave and RF discharges.[2,3] Its three-body rate coefficient has been considered at each moment of the theoretical simulation to depend on the relative concentration of the predominant species N_2O, N_2 and O_2, and their partial contribution as a third body.

The reaction G_6 between NO_2 and oxygen atoms in their fundamental state represents a well-known,[16] very fast channel of NO_2 disappearance in the kinetics of the N_2O discharge, and is mainly responsible for the low NO_2 concentration. In the present model, the NO_2 reaction with oxygen in the metastable state (reaction G_5) has been also included, for the sake of coherence. The rate constant for the reaction[33] is markedly larger than that for the reaction with $O(^3P)$, but given the very small $O(^1D)$ concentration predicted with the model, its contribution to the depletion of NO_2 in the discharge is a very minor one.

Finally, reactions labeled G_7 and G_8 in Table 1, and not considered in ref 1 have been included here: the first one as a very efficient channel of recombination of the NO and N species produced from dissociation processes of N_2O by electronic impact through reaction D_3[2,4] and the second one because of its relatively high rate coefficient in comparison with other processes where NO or $O(^1D)$ are involved, too.

Some attempts have been made to include other chemical reactions in the gas phase, mostly intended to explain the experimental values of the NO_2 concentration. The very encouraging agreement between calculated and measured concentrations for the other stable species found in this work, and their temporal dependencies, are practically insensitive to these minor corrections. In particular, the inclusion of a chain of reactions related with molecular oxygen in the excited state, $O_2(^1\Delta)$, was essayed. In fact, metastable $O_2(^1\Delta)$ is known to be the primary product of the $N_2O + O(^1D) \rightarrow N_2 + O_2$ reaction,[25] since the exit channel producing O_2 in its fundamental state is spin forbidden. On the other hand the rate coefficient of 4.88×10^{-18} cm^{-3} molecule^{-2} s^{-1} at 300 K reported[35] for

the reaction $O_2(^1\Delta) + NO \rightarrow NO_2 + O(^3P)$ is large enough to lead to a significant formation of NO_2 molecules if high concentrations of $O_2(^1\Delta)$ are present. Nevertheless, the $O_2(^1\Delta)$ concentration has been found to decay too quickly by quenching with ground state[36] O_2 or through heterogeneous reactions,[37,38] when included in the model, and the $O_2(^1\Delta)$ chemistry has been disregarded.

Homogeneous reactions among two or three of the stable species involved in the discharge, for example, the well-known reaction[39,40] $2NO + O_2 \rightarrow 2NO_2$ have not been considered in the model, since their reported rate coefficients are many orders of magnitude lower than those of reactions involving atoms and become only important at much larger pressures than those of this work. Other reactions as $NO + NO_2 \rightarrow N_2 + NO_2$ have been studied only at high temperatures,[41,42] but their rate coefficients in the reported interval are too small. Reaction chains involving radicals[41] such as NO_3 or N_2O_5 to produce NO_2 have been also disregarded, since the presence of a significant concentration of these radicals in the hollow cathode N_2O discharge was not observed by infrared spectroscopy in a conclusive way.

Heterogeneous Reactions. Among the heterogeneous reactions considered in the present work, the reactions termed W_1, W_5, and W_6 in Table 1 describe the contribution of the reactor walls to the depletion of the electronically or vibrationally excited levels of oxygen atoms and N_2O molecules appearing explicitly in the model. On the other hand, the reactions labeled W_2, W_3, and W_4 represent the wall recombination of oxygen and nitrogen atoms to form O_2 and N_2, and W_7 contributes to NO_2 generation through the reaction of NO with oxygen atoms adsorbed in the cathode wall. This last reaction was already considered in ref 1 to account approximately for the observed concentration of NO_2 and has been included here, but with a smaller rate constant. At this point, it should be noted that a wrong value of this rate constant (9×10^{-4} cm^3 molecule^{-1} s^{-1}) was listed by mistake in Table 1 of ref 1. The actual rate constant used for that simulations was 6.2×10^{-3} cm^3 molecule^{-1} s^{-1}. When this rate constant is used to simulate the present experimental conditions, a large increase in the NO_2 concentration is predicted after the switching off of the discharge (see Figure 3), which is not observed in the measurements. A reduction of this rate constant to a value of 2.75×10^{-3} cm^3 molecule^{-1} s^{-1} was thus necessary in order to account better for the observations. In any case this is now a minor source of NO_2. As indicated above, in the present model, it is the homogeneous reaction G_3 the one assumed to be responsible for most of the NO_2 concentration.

The reaction W_4 involving nitrogen atoms has been added here as alternative decay channel to the disappearance of this atomic species. The rate coefficients for the reactions involving oxygen atoms W_1 and W_2 are slightly larger when considering the probability per individual collision[2,3] of deexcitation or sticking, $\gamma = 1$, wall recombination and geometrical considerations,[1] than when considering the diffusion-limited case,[43] $k_d = D/\Lambda^2$, with D the diffusion coefficient and Λ the characteristic diffusion length of the cell, which is essentially dependent on the cathode radius. This fact indicates that O atoms diffuse slightly slower than they recombine in the walls, so these reactions have been considered diffusion limited. Deexcitation of N_2O molecules by wall collision has been assumed also to happen with a high probability, next to one, but these processes (reactions W_5 and W_6) are diffusion-limited too, since being a heavier species, the N_2O diffusion coefficient is even smaller than that of oxygen atoms. In contrast, the fraction of $O(^3P)$ wall collisions on stainless steel leading to recombination[44] is markedly smaller than that of the former processes, $\gamma = 4.2 \times 10^{-3}$ at 300 K, and a similar behavior is observed for the fraction of N atoms which collide with the wall to generate N_2 molecules, $\gamma = 3.5 \times 10^{-4}$; therefore, the rate coefficients for reactions W_3 and W_4 are some orders of magnitude smaller than those corresponding to the diffusion limit and are estimated with the following expression:[45]

$$k_{x,wall}[X]V_x = [X]\,\bar{\omega}_x\,\gamma_x\,A/4$$

where A is the reactive wall area, $\bar{\omega}_x$ the mean molecular velocity, and V_x the volume occupied by the X species.

At this point, some remarks should be made about the spatial distribution of the species in the hollow cathode discharge. In the present model, the reaction volume for all the stable molecular species involved in the process has been assumed to be the whole cell volume, so the assumption that the reagents are well mixed is included implicitly. To evaluate this assumption, the characteristic diffusion time $\tau_d = k_d^{-1}$ of each species in N_2O was estimated.[1,43] In our case, with 2 mbar of N_2O in the hollow cathode discharge cell, one gets $\tau_d \approx 2$ ms for the diffusion of N_2O and NO_2 and even smaller values for the lighter diatomic products. This characteristic τ_d is much shorter than the duration of the transient effects to be studied, and smaller than the residence times ($\tau_p \approx 47$ ms to 4.7 s) for all the gas flow rates considered ($\phi = 3-300$ sccm), so diffusive transport dominates over convection by pumping and the reactor can be considered effectively well mixed. Nevertheless, the $O(^1D)$ atoms deexcite or react in a very fast way by collisions with N_2O and other stable species, with typical deexcitation times of some microseconds; during this time interval, $O(^1D)$ diffuses on average less than 1 mm, a distance considerably smaller than the characteristic diffusion length; therefore, the reaction volume for this species has been assumed to be that of the plasma, and the diffusion term involving $O(^1D)$ turns out to be of minor significance. A similar behavior is found for atomic nitrogen and vibrationally exited N_2O; all of them quench or react too fast to diffuse effectively outside the plasma volume, and the effect of their heterogeneous reactions is actually unimportant.

The disappearance of $O(^3P)$ atoms by homogeneous reactions is not so fast as that of $O(^1D)$, but has characteristic times in the millisecond range, similar to the time employed by this species to diffuse up to the cathode wall, and an effective $O(^3P)$ volume similar to that of the cathode could be considered in principle. Nevertheless, the disappearance of $O(^3P)$ by adsorption at the cathode wall and subsequent chemical reaction with new colliders is known to be very efficient, so that the effective $O(^3P)$ concentration is close to zero near the cathode surface[43] and a significant gradient of $O(^3P)$ density should be assumed from the plasma volume to the cathode wall; however, for the sake of simplicity, the reaction volume for this species has been assumed to be that of the plasma too, although the diffusion term has more importance in this case.

Differential Equations. The set of coupled differential equations obtained from the reactions included in Table 1 has been numerically solved by means of a fourth-order Runge−Kutta method. The solution of this set of equations yields the time evolution of the concentrations of each species from the beginning of the discharge to the attainment of the stationary state and from the following extinction of the discharge until the recovery of the original conditions.

For the sake of simplicity, the electron density is assumed to be homogeneous in the plasma volume and negligible outside this region; this plasma volume displays a cylindrical geometry

and is located fundamentally in the middle of the cathode, as experimentally demonstrated in ref 1 for the continuous discharge. In comparison with the time scales relevant for this work, the electron density and energy distributions are assumed to appear and disappear instantaneously upon turning on and off the discharge, in agreement with some literature measurements,[9] where transients of some tens of microseconds are reported for the establishment of the stationary state of the electronic distributions in hollow cathode discharges.

Besides the five stable molecular species N_2O, N_2, O_2, NO, and NO_2, and the transient species $O(^1D)$, $O(^3P)$, N, $N_2O(001)$, $N_2O(100)$, appearing in the gas phase or adsorbed on the cathode wall, the model takes into account the overall mass balance, M, in such a way that the sum of concentrations of all the species equals that predicted by the ideal gas law and allows the estimation of the total pressure in the reactor at each moment. The pressure variation in the discharge cell determines the variation in the output conductances of the experimental system, which were previously calibrated with pure N_2O for different pressures and flow rates. As it was indicated in ref 1, this dependence had to be incorporated into the model for the precise estimation of the temporal dependence of residence times (τ_p), because it influences very remarkably the process of removal by pumping of each stable species, especially at low flow rates. On the contrary, since the rates at which the transient species disappear by gas-phase reactions and heterogeneous recombination are many times larger than the rate at which they are pumped, the inclusion of a pumping term in the respective differential equations has been verified to be irrelevant.

4. Results and Discussion

In Figures 1 and 2 the results of the present chemical kinetics model are compared with the experimental measurements obtained in this work with FTIR and mass spectrometric techniques for the switching on and off of the discharge.

Figure 1a,b shows the experimental absolute concentrations of N_2O in its ground state and NO and NO_2 products obtained by time-resolved rapid scan FTIR absorption spectroscopy, in addition to the model predictions for the modulated discharge, at two, very different gas flow rates: 3 and 108 sccm, respectively. Figure 2 shows the time-resolved mass spectrometric results of N_2 and O_2 for a 3 sccm N_2O flow rate, normalized to the absolute concentrations predicted by the model. In the results for the slower flow (Figures 1a and 2), the concentrations of all the species produced in the discharge show a steep increase after switching on, and a slow decrease when the discharge is turned off. In the case of the faster flow (Figure 1b) the time evolution of the concentrations resembles more closely the square shape of the electrical discharge. As can be seen from Figure 1a,b, the agreement between experimental and calculated data is very good for the precursor, N_2O, and for the NO product, both in the absolute values and in the temporal behavior; and it is qualitatively encouraging for the minor NO_2 product although in this last case the absolute concentration values predicted by the model are smaller than the measured ones. The agreement shown in Figure 2 for the measured and predicted temporal evolution of the homonuclear species is also quite satisfactory.

Concerning Figure 1a, some interesting facts should be noted. At the beginning of the discharge, the concentrations of NO and NO_2 increase suddenly until a maximum value and then decrease rapidly, reaching a plateau ~500 ms after the peak, corresponding to the stationary state with discharge on, and when the discharge is switched off the concentration values of both species decrease slowly. Nevertheless, this sudden peak at the ignition of the discharge is not observed in the time evolution of the concentration of the other two stable products, O_2 and N_2, as it is shown in Figure 2. In Figure 1b it can be seen that the former behavior with a sudden maximum is also not observed for the nitrogen oxides when the gas flow rate is considerably higher than that employed in Figure 1a; on the contrary, the two respective stationary states, discharge on/off, are reached very quickly.

To reproduce theoretically such features, the inclusion of electron impact dissociation terms for both nitrogen oxides in the kinetic model, which were not considered in the previous study of the DC discharge,[1] turns out to be crucial, specially regarding the NO behavior, since without it, a much smoother evolution would be obtained. However, the NO stationary concentrations obtained in the N_2O discharge are not so sensitive to these dissociation terms. Analogously, the smoother temporal behavior of O_2 and N_2 observed in Figure 2 may be attributed to the fact that, once generated, they do not react with the transient species, as the nitrogen oxides do, and hardly dissociate, since their dissociation coefficients by electronic impact should be either very small or negligible under the present conditions. On the other hand, the inclusion of the third N_2O dissociation channel D_3 to give NO + N, followed by the fast reaction G_7 between both species to give $N_2 + O(^3P)$, turns out not to be significant for the sudden increase and depletion of NO observed at the beginning of the discharge, since it has been demonstrated by simulation that both terms equilibrate in less than 1 ms.

The NO_2 generation is dominated by the homogeneous reaction, G_3, and therefore, its time evolution (see Figure 1a) depends on the evolution of the $N_2O(001)$ and $O(^1D)$ concentrations involved in that reaction, which are larger at the beginning of the discharge, as it is shown in Figure 4, where the time dependence of all the species considered in the model are drawn. On the other hand, once the discharge is turned off, a slight but noticeable increase in the experimental NO_2 concentration can be observed, so that NO_2 depletion begins in fact two or three seconds after the discharge has been extinguished and not just in the turn off instant, in contrast with NO, O_2 and N_2 (Figures 1a and 2), which begin to disappear immediately by the action of the exit gas flow. This effect can be traced back to the heterogeneous recombination of NO with oxygen atoms adsorbed in the wall, W_7, which is responsible for the delayed generation of NO_2. As mentioned above, this source of NO_2 was already assumed in the previous model developed for the steady-state discharge but as shown in Figure 3 the value of the rate constant (6.2×10^{-3}) used in ref 1 is too large and gives rise to an exaggerated growth of NO_2 after the discharge has been switched off. In the present model, the contribution of this reaction to the stationary concentration of NO_2 has been relatively diminished by using a smaller rate constant. The other source of NO_2 contemplated in ref 1 is the three body reaction: $O(^3P) + NO + M$, with a well-known rate constant[2,3] and also included in the present model as reaction G_4.This and the heterogeneous reaction alone lead to a too slow rise in the concentration of NO_2 at the beginning of the discharge, and a faster process like the homogeneous reaction G_3, not included in the previous model, becomes necessary in order to approach better the experimental observations. It should be pointed out here that rejecting contributions of the most dubious reactions (i.e., those for which no direct information is available in the literature) G_3 and W_4 to the kinetics and leaving only the contribution of the best established reaction G_4 as the only NO_2

source[2,3] results in NO_2 concentrations some 3 orders of magnitude lower than the data experimentally obtained in this work.

Besides the agreement of the present kinetic model with the experimental results of the modulated N_2O hollow cathode discharge, the validation of the present model would require a good agreement between the calculations and the stationary data from the continuous discharge. Figure 5 shows the experimental data obtained for the stationary concentrations of the stable compounds involved in a 2 mbar continuous N_2O discharge, and the predictions of the present model. This figure may be compared with Figure 5 of ref 1, where the results of the former simplified model were displayed. Although the agreement between calculated and experimental concentrations of the major species of the discharge, N_2O, N_2, O_2, and NO was encouraging in ref 1, it can be observed that this agreement is even better with the present theoretical data. Particularly, NO concentrations fit the experimental results in a more accurate way at low flow rates than they did in the former article, and the homonuclear molecules fit it slightly better at the highest flow rates. On the other hand, the predicted NO_2 concentration dependence on flow rate agrees much better than before with the DC experimental results. All these facts lead us to the conclusion that the present model is more suitable to reproduce the N_2O hollow cathode discharge.

Together with the stable species, Figure 5 shows the stationary concentrations calculated for the transient species appearing explicitly in the current model, such as the atoms and the excited N_2O molecules. It was not possible to detect these species experimentally either by absorption spectroscopy or mass spectrometry under the present conditions. Nevertheless, the FTIR emission spectra of a 45 Hz modulated, N_2O discharge, obtained by phase-sensitive detection techniques at intermediate gas flow rates (36 sccm)[7] and spectrally calibrated with a blackbody source, allowed an estimate of the intensity of the ν_3 vibrorotational band, and the temperature of the (001) vibrational level, which turned out to be ~1300 K. This fact implied a N_2O population of this level ~9%, which is in very satisfactory agreement with the predictions of the present model. Similarly, N_2O excited to the (100) vibrational level is predicted by the model to be populated between 2 and 3 orders of magnitude less than the N_2O ground state, depending of the gas flow rate, as shown in Figure 5. As it was formerly explained, the (100) state of N_2O is known to quench and depopulate much more efficiently than the (001) state, and hence vibrational temperatures only slightly higher than the ambient value are experimentally found in the literature for (100).[11] For a 300 K temperature, a ~0.2% population of the (100) level can be estimated in relation with the fundamental state, assuming a Boltzman distribution, while a 400 K temperature implies a (100) population of ~1%. These values agree quantitatively in a very encouraging way with those estimated by the present model.

5. Summary and Conclusions

In this work the transient processes which happen around the ignition and extinction of a low frequency, square wave modulated, hollow cathode discharge of N_2O until the attainment of the respective stationary states have been studied for the first time. To follow the evolution of the absolute concentrations of the stable nitrogen oxides, time-resolved rapid-scan FTIR absorption spectroscopy has been employed; complementarily, time-resolved mass spectrometry has allowed to know the evolution of the homonuclear molecular species, nitrogen and oxygen, generated at the discharge. To rationalize the collected set of data, a relatively simple chemical kinetics model including a reduced number of reactions is proposed. The corresponding set of coupled, time dependent, differential equations has been numerically solved and the time-resolved solutions compared with the measurements. This model has been also compared with the steady-state experimental results obtained with a DC hollow cathode discharge. The fitting of the simulated transient phenomena to the measured ones has proven to be much more sensitive to the suitable choice of the particular kinetic processes than the stationary studies performed on DC discharges, or based on RF or microwave discharges applied in a continuous way. The present work demonstrates thus the great usefulness of time-resolved studies on low-frequency modulated discharges for the elucidation of the influence of relevant kinetic mechanisms in the plasma chemistry.

A considerable effort has been devoted to the identification of the possible reactions generating NO_2 in the discharge cell, because the rate coefficients of the reactions available in the kinetic databases and in the literature could not justify the relatively high concentration of this species found in the N_2O hollow cathode discharge. In this way, the delayed depletion of NO_2 concentration once the discharge has been extinguished, a feature that has not been observed for the other stable products of the discharge, seems to confirm the occurrence of a heterogeneous reaction generating NO_2 molecules, which was proposed by Arcos et al.;[1] nevertheless, to reproduce more suitably the temporal evolution of NO_2 at the beginning of the discharge and the general behavior of the DC discharges for different physical conditions, a large enhancement of the rate constant of the bimolecular reaction $O(^1D) + N_2O \rightarrow NO_2 + N$ by the long-lived vibrationally excited $N_2O(\nu_3)$ molecules has been proposed for the first time. This reaction decreases the relative significance of NO_2 generation by wall reaction.

To justify the temporal behavior of the rest of the stable products at the beginning of the discharge, dissociation processes by electron impact have been incorporated into the model, this fact being specially decisive for NO, which seems to dissociate in a much more efficient way than N_2 and O_2.

The inclusion of vibrational N_2O excitation processes and relaxation channels in the kinetics model, specially for the (001) state, justify the fact that the N_2O signals obtained by FTIR absorption spectroscopy are not exactly due to the total N_2O concentration, but to ground-state N_2O molecules, which under the present experimental conditions may differ by some ten percent from the total density of N_2O molecules.

The agreement between the model predictions and the experimental data for the N_2O, N_2, O_2, and NO is good. The calculations can also reproduce satisfactorily the qualitative behavior of the minor NO_2 product and, although the values obtained are still low, the predictions of the model are closer, by several orders of magnitude, to the absolute concentrations observed for this molecule than those of other models described in the literature. This general agreement between calculations and experiment, both time-resolved and in the steady state, suggests that the model provides a reasonable global description of the processes performed on the hollow cathode N_2O discharge.

Acknowledgment. We are indebted to J. L. Domenech, who wrote the program for the simulation of the spectra. The technical advice and support of J. M. Castillo, M. A. Moreno, and J. Rodríguez have been most valuable for the achievement of the present experiments. The SEUID of Spain (Projects PB95-

0918-C03-02 and PB96-0881) is gratefully acknowledged for financial support.

References and Notes

(1) Arcos, T.; Domingo, C.; Herrero, V. J.; Sanz, M. M.; Schulz, A.; Tanarro, I. *J. Phys. Chem. A* **1998**, *102*, 6282.
(2) Cleland, T. A.; Hess, D. W. *J. Electrochem. Soc.* **1989**, *136*, 3103.
(3) Kline, L. E.; Partlow, W. D.; Young, R. M.; Mitchell, R. R.; Congedo, T. V. *IEEE Trans. Plasma Sci.* **1991**, *19*, 278.
(4) Ung, A. Y. M. *Chem. Phys. Lett.* **1975**, *32*, 351.
(5) Piper, L. G.; Rawlins, W. T. *J. Phys. Chem.* **1986**, *90*, 321.
(6) Arcos, T.; Castillo, M.; Domingo, C.; Herrero, V. J.; Sanz, M. M.; Schulz, A.; Tanarro, I. To be published.
(7) Arcos, T. Espectroscopía y dinámica de plasmas de N_2O en descargas de cátodo hueco. Ph.D. Thesis, Madrid, 1998.
(8) Rothman, L. S. *J. Quant. Spectrosc. Radiat. Transfer.* **1992**, *48*, 469.
(9) Arslanbekov, R. R.; Kudryavtsev, A. A. *Proceedings of the NATO Advanced Research Workshop on Electron Kinetics and Applications of Glow Discharges*; Kortshagen, U., Tsedin, L. D., Eds.; NATO ASI Series Book; Plenum: New York, 1998.
(10) Bates, R. D., Jr.; Flynn, G. W. *J. Chem. Phys.* **1968**, *49*, 1432.
(11) O'Neil, J. A. *J. Vac. Sci. Technol. A* **1991**, *9*, 669.
(12) Radzig, A. A.; Smirnov, B. M. *Reference Data of Atoms, Molecules, and Ions*, Springer-Verlag: Berlin, **1985**.
(13) Penetrante, B. M.; Hsiao, M. C.; Bardsley, J. N.; Merrit, B. T.; Vogtlin, G. E.; Kuthi, A.; Burkhart, C. P.; Bayless, J. R. *Plasma Sources Sci. Technol.* **1997**, *6*, 251.
(14) Huddleston, R. K.; Weitz, E. *J. Chem. Phys.* **1981**, *74*, 2879.
(15) Hayashi, M.; Niwa, A. *Proceedings of the Fifth International Symposium on Gaseous Dielectrics*; Christophorou, L. G., Ed.; Pergamon: New York, 1987.
(16) Atkinson, R.; Baulch, D. L.; Cox, R. A.; Hampson, Jr. R. F.; Kerr, J. A.; Rossi, M. J.; Troe, J. *J. Phys. Chem. Ref. Data* **1999**, *28*, 191.
(17) McEwan, M. J.; Phillips, L. F.*Chemistry of the Atmosphere*; John Wiley and Sons: New York, 1975.
(18) Murphy, R. E.; Cook, F. H.; Sakai, H. *J. Opt. Soc. Am.* **1975**, *65*, 600.
(19) Arnold, J. W.; McCoubrey, J. C.; Ubbelohde, A. R. *Proc. R. Soc.* **1958**, *A248*, 445.
(20) Yardley, J. T. *J. Chem. Phys.* **1968**, *49*, 2816.
(21) Farrenq, R.; Dupre-Maquaire, J. *J. Mol. Spectrosc.* **1974**, *49*, 268.
(22) Yardley, J. T. *Introduction to Molecular Energy Transfer*; Academic Press: London, 1980.
(23) Chase, M. W., Davies, C. A., Downey, J. R., Frurip, D. J., McDonaald, R. A., Syverud, A. N., Eds. *JANAF Thermochem Tables*, 3rd ed; U. S. National Bureau of Standards: Washington, DC, 1985.
(24) Donovan, R. J.; Husain, D. *Chem. Rev.* **1970**, *70*, 489.
(25) Last, I.; Aguilar, A.; Sayós, R.; Gonzáles, M.; Gilibert, M. *J. Phys. Chem. A* **1997**, *10*, 1206.
(26) Davison, J. A.; Carleton, J. H.; Schiff, H. I.; Fehsenfeld, F. C. *J. Chem. Phys.* **1979**, *70*, 1697.
(27) Bernstein, R. B. *State to State Chemistry*; Brooks, P. R., Hayes, E. F., Eds.; ACS Symposium Series 56; American Chemical Society: Washington, DC, 1977.
(28) Levine, R. D.; Bernstein, R. B. *Molecular Reaction Dynamics and Chemical Reactivity*; Oxford University Press: Oxford, 1987.
(29) Aoiz, F. J.; Herrero, V. J.; Sáez Rábanos, V. *J. Chem. Phys.* **1991**, *94*, 7991.
(30) Aoiz, F. J.; Bañares, L.; Díez-Rojo, T.; Herrero, V. J.; Sáez Rábanos, V. *J. Phys. Chem.* **1996**, *100*, 4071.
(31) Aoiz, F. J.; Bañares, L.; Herrero, V. J.; Sáez Rábanos, V.; Tanarro, I. *J. Phys. Chem.* **1997**, *101*, 6165.
(32) Clary, D. C. *J. Phys. Chem.* **1994**, *98*, 10678.
(33) Gauthier, M. J. E.; Snelling, D. R. *J. Photochem.* **1975**, *4*, 27.
(34) Atkinson, R.; Baulch, D. L.; Cox, R. A.; Hampson, R. F., Jr.; Kerr, M. J.; Troe; J. *J. Phys. Chem. Ref. Data* **1989**, *18*, 881.
(35) Dumas, J. L. *Bull. Soc. Chim. Fr.* **1976**, 658.
(36) Okabe, H. *Photochemistry of Small Molecules*; Wiley and Sons: New York, 1978.
(37) Findlay, F. D.; Snelling, D. R. *J. Chem. Phys.* **1971**, *55*, 545.
(38) Crannage, R. P.; Dorko, E. A.; Johnson, D. E.; Whitefield, P. D. *Chem. Phys.* **1993**, *169*, 267.
(39) Olbregts, J. *Int. J. Chem. Kinet.* **1985**, *17*, 835.
(40) Shaaban, A. F. *J. Chem. Educ.* **1990**, *67*, 869.
(41) Westley, F., Herron, J. T., Hampson, R. F., Mallard, W. G., Eds.; NIST Standard Reference Database 17, NIST Chemical Kinetics Database, Version 4.0; National Institutes of Standards and Technology: Gaithersburg, MD, 1992.
(42) Gvozdev, A. A.; Nesterenko, V. B.; Nichipor, G. V.; Trubnikov, V. P. *Vestsi Akad. Navuk BSSR, Ser. Fiz. Energ. Navuk* **1979**, 73.
(43) Chantry, P. J. *J. Appl. Phys.* **1987**, *62*, 1141.
(44) Morgan, J. E.; Schiff, H. I. *U.S. Government Research and Development Report;* U.S. Government Printing Office: Washington, DC, **1966**; Vol. 5, 67.
(45) Sabadil, H.; Pfau, S. *Plasma Chem. Plasma Process.* **1985**, *5*, 67.